Determination of an analytical relation for binding energy dependence on small size silicon nanoclusters ($n_{Si} \leq 10$ at.)

ABDELLAZIZ DOGHMANE, LINDA ACHOU[*], ZAHIA HADJOUB
Laboratoire des Semi-conducteurs, Département de Physique, Faculté des Sciences, Université Badji-Mokhtar, Annaba, BP 12, DZ-23000, Algeria

As there is no a universal theoretical method nor an accepted single model to predict the relation between size, n_{Si}, and interatomic binding energy, E_b, in Si nanoclusters, we developed an original approach combining the most used computational methods to deduce a unique relation for small Si nanoclusters ($n_{Si} \leq 10$ atoms). We first determine the mean relation for each category, then for all of them. It is found that the mean analytical E_b-n_{Si} relation takes the form, $E_b = C + \alpha \exp(-n_{Si}/\beta)$ where C, α, and β are constants deduced for each method. Then, a unique relation for all theoretical methods was found to be $(E_b)_{Si} = 3.73 - 6.29 \exp(-n_{Si}/2.03)$. Finally, the validity of this expression is tested. We show that this formula is applicable to all methods for any number of Si atoms. Knowing the size of the aggregates, one can deduce the binding energy and vice-versa.

1. Introduction

Among many categories of low-dimensional systems, acting as building blocks for modern nanodevices, silicon atomic clusters (Si ACs) with different sizes, shapes and compositions are the most appropriate [1-5]. They exhibit a rich variety of properties, which lie between those of individual atoms and the properties of condensed matter, therefore they differ from their microscopic and macroscopic counterparts [6, 7]. The analysis of the binding energy of isolated Si_n clusters is of great interest for many reasons. First, the binding energy is the key material property reflecting the cluster's stability. Second, it is one of the intrinsic parameters of each material: in macroscopic systems, it is constant (4.63 eV) [8], but at the nanometer scale E_b depends on the size. Finally, the determination of the binding energy leads to a better understanding of other materials characteristics such as the thermodynamical and mechanical properties. However, there is a great lack of experimental data at the nanoscale regime because of the difficulty to obtain them [9]. Consequently, there is a strong need for simple theoretical equations to determine nano-parameters in order to overcome and remediate such difficulties.

In this context, we present an original approach for evaluating the binding energy in terms of a size for small Si clusters composed of up to 10 atoms. The study is based on the most widely used computational methods: (i) non-empirical model solving the Schrodinger equation [10], (ii) semi-empirical, and (iii) empirical calculating methods. First, we deduce, for every case, a mean analytical E_b-n_{Si} relation, then we determine a unique expression for all theoretical methods. Finally, we test the validity of the obtained expression by comparing with the experimental data.

2. Materials and methodology

2. 1 Structural properties of the clusters

The characteristics of Si_n ACs are radically different from those of the same material in its bulk form. They show, in general, several differences which are: (i) high proportion of atoms at the surface, (ii) absence of the tetrahedral coordination, and (iii) deviation of the Si-Si interatomic distance out of 2.35 Å. These new characteristics lead to interesting properties which are different than those of the bulk of a silicon solid [11].

2.2 Computational approach

Despite the great number of proposed non-empirical, semi-empirical, and empirical computational methods, there is neither a unique theoretical method nor a single model to predict the relation between size and interatomic binding energy in Si nanoclusters. That's why the combination of all of them would be a good approach to

reach this goal. The procedure consists of the following steps:

(i) Data choice: Survey, select, and exploit the binding energy data calculated by the frequently used theoretical methods reported in the literature;

(ii) Quantification of size effects on E_b: Plot the data as a function of n_{Si} (with $n_{Si} \leq 10$ at.) and then determine an analytical relation $E_b = f(n_{Si})$;

(iii) Generalization of $E_b = f(n_{Si})$: Such relations are generalized for each calculating method (non-empirical, semi-empirical, and empirical);

(iv) Validity of the E_b expression: Test the validity of the obtained relation by comparing it to experimental data.

3. Results and discussion

3.1 Quantification of size effects on binding energy using non-empirical methods

3.1.1 Hartree-Fock (HF) and Post-HF methods

To investigate quantitatively Si_n energetic stabilities and their dependence on various post-HF methods, we concentrate on low dimension clusters ($n_{Si} \leq 10$ at.) where the size effects are very important. The obtained results are shown in Fig. 1, where the binding energy per atom (E_b/at.) is presented as a function of the number of atoms (n_{Si}).

Post-HF calculations are classified by the following levels of theory: (i) The MP4/6-31G*[1], MP2/6-31G(d) [2], MP2/aug-cc-pVTZ [12] methods using a Møller–Plesset formulation for the correlation energy and a valence double-zeta sp plus a set of d-type polarization functions, a standard split valence with polarization functions, an augmented correlation consistent polar valence triple zeta for the basis sets, respectively, (ii) The coupled-cluster single and double substitutions (including triple excitations) (CCSD (T)/6-31G(d)) model [4, 13].
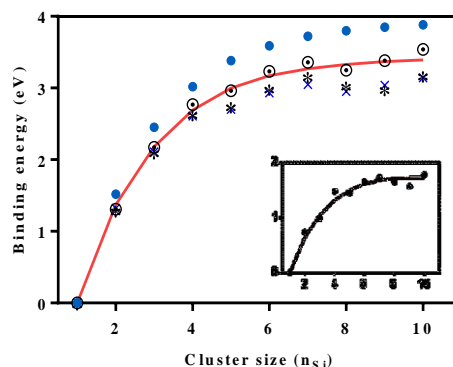

*Fig. 1. Binding energy vs. cluster size for small Si_n calculated with Post-HF methods: *: MP4/6-31G*[1], ○: MP2/6-31G(d) [2], ●: MP2/aug-cc-pVTZ [12], and ×: CCSD (T)/6-31G(d) [4, 13]. The Continuous line: —— represents the best mean approximation fit. Inset shows E_b vs. n_{Si} calculated by HF/6-31G* [1].*

It can clearly be seen that the general trend of the E_b-n_{Si} curves obtained by Post-HF techniques is characterized by a rapid initial increase ($n_{Si} \leq 5$) followed by a tendency towards saturation for higher atom numbers. Such a behavior can be expressed by an exponential dependence obtained via curve fitting:

$$E_b = C + \alpha \exp(-n_{Si}/\beta) \qquad (1)$$

where C, α, and β are characteristic constants deduced for each method. The values of these constants (and their calculated standard errors, SE) are regrouped in Table 1. From their mean values one can deduce a mean relation describing the dependence of E_b on n_{Si}:

$$(E_b)_{Post-HF} = 3.42 - 5.80 \exp(-n_{Si}/1.90) \qquad (2)$$

To test the validity of this mean approximation, we superimpose the calculated curve (Eq. 2), plotted as solid line, on the plotted data of the four methods in Fig. 1. The agreement is quite good as evidenced by the standard errors which are very close to zero.

Table 1. Deduced values of C, α, and β for Si_n clusters calculated using post-HF methods. Numbers in ( ) represent the SE.

Post-HF	MP2	MP2	MP4	CCSD(T)	**Mean values**
Basis sets (BS)	aug-cc-pVTZ	6-31G (d)	6-31G*	6-31G(d)	
C	3,93 (0.0019)	3.49 (0.0492)	3.15 (0.0489)	3.09 (0.0356)	**3.42 (0.0139)**
α	-6,41 (0.0076)	-5.74 (0.2017)	-5.56 (0.2653)	-5.49 (0.2004)	**-5.80 (0.0065)**
β	2,04 (0.0039)	2.03 (0.1145)	1.78 (0.1200)	1.75 (0.0889)	**1.90 (0.0033)**

It is worth noting that the HF/6-31G* (in the inset of Fig. 1), considered as the basic ab initio methods, has the same exponential behavior as that presented by advanced HF methods.

3.1.2 Density functional theory (DFT) methods

The influence of cluster size on binding energy calculated via several DFT methods is plotted in Fig. 2 (a-c) for:

(i) Local density approximation (LDA) with Ceperley and Alder (C-A) [2], full-potential (FP) [3], Vosko-Wilk-Nusair (VWN) [4, 14], Perdew-Wang and Vosko-Wilk-Nusair (PW-VWN) [15], Post Local-Spin-Density (PLSD)

[16], Perdew-Burke-Ernzerhof (PBE) [17] methods using plane-wave (PW) [2], linear muffin-tin orbital (LMTO) [3], Even-Tempered which consists of 8s6p3d1f and is of quadruple z quality and with three polarization functions (ET-QZ3p) [4], Double Numerical Polarized (DNP) [14], triple zeta plus polarization (TZP) [15], PW [16], 6s5p3d [17] basis sets, respectively.

(ii) Generalized Gradient Approximation (GGA) with Becke and Lee-Yang-Parr (BLYP) [4], Perdew-Wang-Becke 88 (PWB) [14], Perdew-Wang 91 (PW91) [18, 19, 20], Perdew-Burke-Ernzerhof (PBE) [21], revised Perdew-Burke-Ernzerhof (RPBE) [22] methods using ET-QZ3p [4], DNP [14, 18], 6-311++G(2d) [19], double numerical basis including d-polarization functions (DND) [20, 22], Projector-Augmented-Wave (PAW) [21] basis sets and/or pseudopotentials.

(iii) Hybrid methods with Becke's three-parameter and Lee-Yang-Parr (B3LYP) method [4, 19, 23-25] using 6-311G* [4], 6-311++G(2d) [19], Los Alamos National Laboratory 2 double zeta (LanL2DZ) [23], 6-31G(d) [24], 6-311+G(d) [25] basis sets and Becke's three-parameter Perdew-Wang (B3PW91) method with LanL2DZ [26] basis set.

In Fig. 2 (a-c) we can observe that all the curves show a similar behavior to the one observed for HF and Post-HF methods. Thus, the E_b dependence on n_{Si} could also be expressed by an exponential relation. In the Table 2, are included the mean values of constants from which the following quantified $E_b = f(n_{Si})$ relations are determined:

$$(E_b)_{LDA} = 4.17 - 7.59 \exp(-n_{Si}/1.66) \qquad (3)$$

$$(E_b)_{GGA} = 3.56 - 6.60 \exp(-n_{Si}/1.61) \qquad (4)$$

$$(E_b)_{Hybr.} = 3.41 - 7.08 \exp(-n_{Si}/1.42) \qquad (5)$$

We notice that these mean approximations which are plotted as solid lines in Fig. 2 (a-c), are in good agreement with all DFT variants.

In order to obtain a general relation of DFT methods, we plot in Fig. 2d the curves deduced from equations (3), (4), and (5). The mean values of C, α, and β were found to be: $C_{mean} = 3.71$ (SE = 0.0021), $\alpha_{mean} = -7.09$ (SE = 0.0149) and $\beta_{mean} = 1.56$ (SE = 0.0043) leading to the following relation, plotted in Fig. 2d as a continuous curve:

$$(E_b)_{DFT} = 3.71 - 7.09 \exp(-n_{Si}/1.56) \qquad (6)$$

A standard error ≤ 0.01 means we are very close to our targeted approximation, which is good.
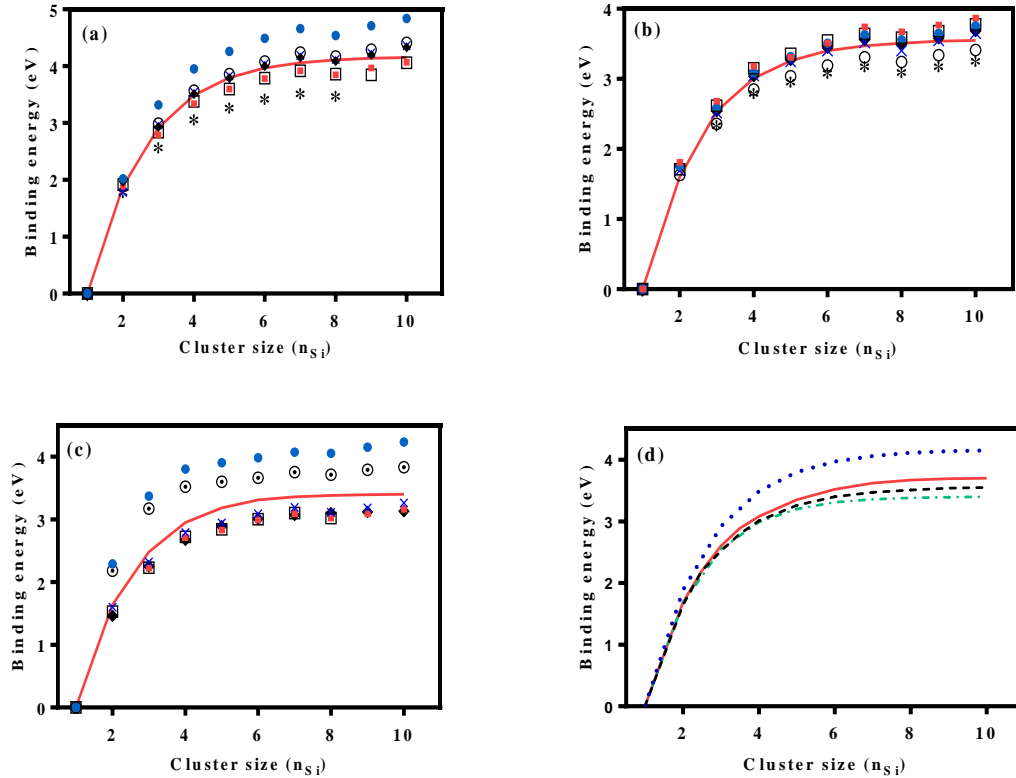

Fig. 2. Binding energy vs. cluster size for small Si_n calculated with DFT methods: (a) LDA: ■: CA/PW [2], ●: FP/LMTO [3], ○: VWN/ET-QZ3p [4], ♦: VWN/DNP [14], *: PW-VWN/TZP [15], □: PLSD/PW [16], ×: PBE/6s5p3d [17], (b) GGA: *: BLYP/ET-QZ3p [4], ♦: PWB/DNP [14], □: PW91/DNP [18], ●: PW91/6-311++G(2d) [19], ×: PW91/DND [20], ■: PBE/PAW [21], ○: RPBE/DND [22], (c) hybrids: ■: B3LYP/6-311 G* [4], ×: B3LYP/6-311++G(2d) [19], ○: B3LYP/LanL2DZ [23], ♦: B3LYP/6-31 G(d) [24], □: B3LYP/6-311+G(d) [25], ●: B3PW91/LanL2DZ [26], and (d) Comparative study of DFT methods: ⋯⋯: LDA (Eq. 3), − − −: GGA (Eq. 4) and − · − · : hybrids (Eq. 5). The continuous lines: —— represent the best mean approximations fit and indicate the analytical predictions of Eqs. (3-6).

Table 2. Deduced values of C, α, and β for Si_n calculated using LDA, GGA, and hybrid methods. Numbers in ( ) represent the SE.

LDA	FP	VWN	VWN	PBE	C-A	PLSD	PW-VWN	Mean
BS	LMTO	ET-QZ3p	DNP	6s5p3d	PW	PW	TZP	values
C	4.77 (0.0433)	4.34 (0.0355)	4.24 (0.0353)	4.30 (0.0367)	3.99 (0.0319)	3.96 (0.0342)	3.56 (0.0284)	**4.17 (0.0013)**
α	-8.52 (0.2487)	-7.68 (0.1928)	-7.60 (0.2104)	-7.61 (0.2015)	-7.27 (0.2021)	-7.46 (0.2430)	-6.99 (0.1752)	**-7.59 (0.0079)**
β	1.73 (0.0699)	1.75 (0.0671)	1.70 (0.0640)	1.77 (0.0659)	1.65 (0.0608)	1.57 (0.0643)	1.47 (0.040)	**1.66 (0.0023)**
GGA	PBE	PW91	PW91	PW91	PWB	RPBE	BLYP	Mean
BS	PAW	DNP	6-311++G (2d)	DND	DNP	DND	ET-QZ3p	values
C	3.77 (0.0465)	3.72 (0.0242)	3.69 (0.0294)	3.57 (0.0338)	3.61 (0.0306)	3.35 (0.0272)	3.23 (0.0242)	**3.56 (0.0022)**
α	-6.86 (0.2951)	-6.84 (0.1562)	-6.75 (0.1893)	-6.66 (0.2280)	-6.68 (0.2048)	-6.23 (0.1840)	-6.27 (0.1841)	**-6.61 (0.0147)**
β	1.65 (0.0940)	1.64 (0.0492)	1.64 (0.0605)	1.60 (0.0710)	1.61 (0.0639)	1.60 (0.0610)	1.51 (0.0608)	**1.61 (0.0046)**
Hybrid	B3PW91	B3LYP	B3LYP	B3LYP	B3LYP	B3LYP	Mean	
BS	LanL2DZ	LanL2DZ	6-311++G (2d)	6-311 G*	6-31 G (d)	6-311+ G(d)	values	
C	4.12 (0.0299)	3.76 (0.0219)	3.21 (0.0238)	3.12 (0.0261)	3.14 (0.0019)	3.10 (0.0343)	**3.41 (0.0046)**	
α	-9.39 (0.3588)	-9.13 (0.3090)	-6.20 (0.1814)	-5.87 (0.1778)	-5.90 (0.0130)	-6.00 (0.2012)	**-7.08 (0.0375)**	
β	1.21 (0.0482)	1.13 (0.0375)	1.51 (0.0544)	1.58 (0.0681)	1.59 (0.0045)	1.51 (0.0683)	**1.42 (0.0096)**	

3.1.3. Non-empirical methods generalization

In order to generalize the relations obtained above, and then describe the non-empirical methods by only one equation, we plot in Fig. 3, the size effects on $(E_b)_{Post-HF}$, $(E_b)_{DFT}$, and $(E_b)_{DMC}$ with $(E_b)_{DMC} = 3.47 – 6.21 \exp (-n_{Si}/1.71)$ for Diffusion Monte Carlo method. Following the above calculation procedure, we get the following general relation, represented by the continuous line, in the case of ab initio category:

$$(E_b)_{non-empir.} = 3.53 - 6.37\exp (-n_{Si}/1.72) \qquad (7)$$

The standard errors on C, α, and β are 0.0023, 0.0131, and 0.0050, respectively. Therefore, we can conclude that these values are known with a reasonably good precision.
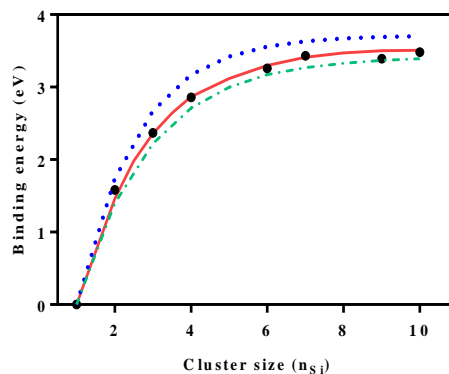

Fig. 3. Comparative study of non empirical methods: − · − · : Post-HF (Eq. 2), ·······: DFT (Eq. 6) and ●: DMC [5] applied to small Si_n. The continuous line: —— indicates the non-empirical theoretical prediction (Eq. 7).

3.2 Quantification of size effects on binding energy using semi-empirical and empirical methods

To enhance the present work and validate the above results that were obtained from non empirical methods (Eq. 7), we consider other classes of methods namely: (i) semi-empirical (Functional based density TB (DFTB) [17], TB [27], Nonorthogonal TB [28], Nonconventional TB (NTB) [29], Austin Model 1 (AM1) [30]) and (ii) empirical potential energy function of Li, Johnston and Murrell (LJM) [31]. Fig. 4 (a and b) regroups some reported data of the binding energy's variation.
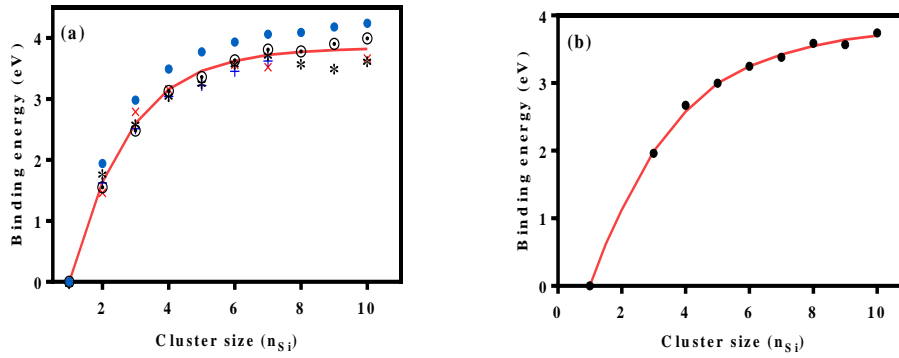
*Fig. 4. Binding energy vs. cluster size for small Si_n calculated with: (a) semi-empirical methods: •: DF-TB [17], *: TB [27], ○: Nonorthogonal TB [28], +: NTB [29], ×: AM1 [30] and (b) LJM potential [31]. The continuous line: —— represents the best fit.*

The deduced mean relations for both semi-empirical (Table 3) and empirical methods are:

$$(E_b)_{semi-empir.} = 3.84 - 6.90 \exp(-n_{Si}/1.73) \qquad (8)$$

$$(E_b)_{empir.} = (E_b)_{LJM} = 3.82 - 5.60 \exp(-n_{Si}/2.63) \qquad (9)$$

Table 3. Deduced values of C, α, and β for Si_n calculated using semi-empirical methods. Numbers in ( ) represent the SE.

Semi-empr.	DF-TB	Nonorthogonal TB	TB	NTB	AM1	**Mean values**
C	4.18 (0.0251)	3.98 (0.0328)	3.66 (0.0499)	3.68 (0.0550)	3.69 (0.1083)	**3.84 (0.0025)**
α	-7.64 (0.1597)	-6.50 (0.1330)	-6.88 (0.3499)	-6.49 (0.1813)	-6.99 (0.5588)	**-6.90 (0.0140)**
β	1.65 (0.0455)	2.04 (0.0674)	1.57 (0.1015)	1.76 (0.0871)	1.61 (0.1781)	**1.73 (0.0050)**

3.3 Determination and validation of a unique E_b-n_{Si} relation

The unique relation for all non-empirical, semi-empirical, and empirical categories can be expressed by the mean values of the characteristic constants deduced above from their energy-size equations, as follows:

$$(E_b)_{Si} = 3.73 - 6.29 \exp(-n_{Si}/2.03) \qquad (10)$$

E_b-n_{Si} for Eq. (10) as well as dependencies for non-empirical, semi-empirical, and empirical categories from relations (7-9) are plotted in Fig. 5 (a). The agreement is quite good and the errors of 0.0092, 0.0349, and 0.0203 are too low, confirming the validity and the acceptability of this approach.

To validate the proposed model (Eq. 10), we plot in Fig. 5 (b) the analytical prediction and the available experimental data in the literature [32]. An excellent theory-experiment agreement is clearly observed.

To estimate the precision of the present theoretical approach (Eq. 10), we calculate discrepancies in (%) relative to binding energy values obtained from experimental method [17] using infrared and Raman spectroscopy, i.e. $\Delta E_b = |E_{b(exp)} - E_{b(theo)}|/ E_{b(exp)}$. The results are very encouraging, as evidenced by the low relative discrepancies (generally $\leq 5\%$).

The best obtained uncertainties are: $\Delta E_b = 0.87\%$ (for $n_{Si} = 6$), $\Delta E_b = 1.54\%$ (for $n_{Si} = 5$), $\Delta E_b = 1.94\%$ (for $n_{Si} = 7$) and $\Delta E_b = 1.98\%$ (for $n_{Si} = 8$).
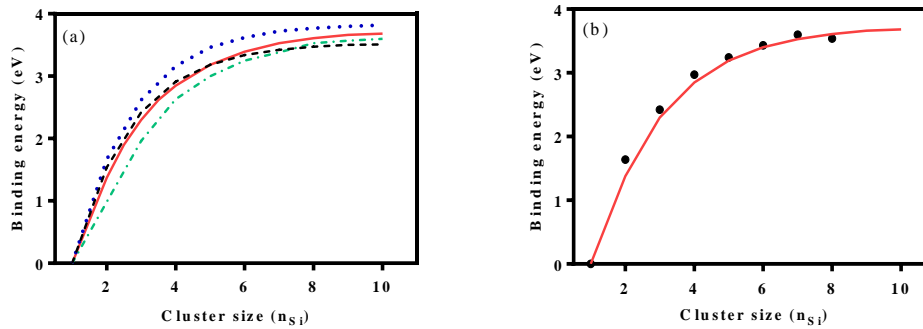

Fig. 5. (a) Plot of deduced relations for all categories: − − −: non-empirical (Eq. 7), ……: semi-empirical (Eq. 8), and − · − ·: empirical (Eq. 9). The continuous line: —— represents the determined unique relation (Eq. 10); (b) Validation of the proposed model (Eq. 10): —— with •: experimental results [32].

The advantage of the present equation lies in the possibility of evaluating the binding energy based on the cluster size. This would be useful for experimental synthesis and technological applications by designing such Si_n with desired E_b to achieve the adequate cohesion which is highly required for materials stability, good operation, and high performance of nanoscale devices.

4. Conclusion

The binding energy dependence on the size of small Si nanoclusters has been investigated. The main results are summarized below:

(i) All the curves show an initial sharp increase ($n_{Si} \leq 5$ at.) followed by a transition region ($5 \leq n_{Si} \leq 10$) that saturates for relatively higher atom number ($n_{Si} > 10$ at.).

(ii) The quantification of the initial increasing regions ($n_{Si} \leq 10$ at.) led to an exponential behavior of the form $E_b = C + \alpha \exp(-n_{Si}/\beta)$ where C, α, and β are characteristic coefficients deduced for each computational method.

(iii) We have shown that the E_b-n_{Si} dependencies are described by a unique relation of the form: $E_b(_{Si}) = 3.73 - 6.29 \exp(-n_{Si}/2.03)$.

(iv) This relation has been found to be in good agreement with experimental data.

References

[1] K. Raghavachari, C.M. Rohlfing, J. Chem. Phys. **89**, 2219 (1988).

[2] C. Majumder, S. K. Kulshreshtha, Phys. Rev. B **69**, 115432-1 (2004).

[3] B. X. Li, P. L. Cao, S. C. Zhan, Phys. Lett. A **316**, 252 (2003).

[4] C. Pouchan, D. Bégue, D. Y. Zhang, J. Chem. Phys. **121**, 4628 (2004).

[5] J. C. Grossman, L. Mitas, Phys. Rev. Lett. **74**, 1323 (1995).

[6] P. Jena, A. W. Castleman, Jr., Nanoclusters: A Bridge Across Disciplines, ed. By P. Jena, A. W. Castleman, (Elsevier, Amsterdam, 2010).

[7] B. Bhushan, D. Luo, S. R. Schricker, W. Sigmund, S. Zauscher, Handbook of Nanomaterials Properties (Springer, Berlin Heidelberg, 2014).

[8] C. Kittel, Introduction to solid state physics, 8th ed. (Dunod, Paris, 2007).

[9] H. Toffoli, S. Erkoç, D. Toffoli, "Modeling of Nanostructures", in Computational Chemistry, ed. By J. Leszczynski, (Springer, New York, 2012).

[10] E. Schrödinger, Ann. Phys. **79**, 489 (1926); E. Schrödinger, Ann. Phys. **79**, 361 (1926).

[11] R. Q. Zhang, in Growth Mechanisms and Novel Properties of Silicon Nanostructures from Quantum-Mechanical Calculations, ed. By R. Q. Zhang (Springer, Berlin Heidelberg, 2014).

[12] S. Nigam, C. Majumder, S. K. Kulshreshtha, J. Chem. Phys. **125**, 074303 (2006).

[13] X. Zhu, X. C. Zeng, J. Chem. Phys. **118**, 3558 (2003).

[14] B. Liu, Z. Y. Lu, B. Pan, C. Z. Wang, K. M. Ho, A. A. Shvartsburg, M. F. Jarrold, J. Chem. Phys. **109**, 9401 (1998).

[15] R. Fournier, S. B. Sinnott, A. E. DePristo, J. Chem. Phys. **97**, 4149 (1992).

[16] S. Wei, R. N. Barnett, U. Landman, Phys. Rev. B **55**, 7935 (1997).

[17] A. Sieck, D. Porezag, Th. Frauenheim, M. R. Pederson K. Jackson, Phys. Rev. A **56**, 4890 (1997).

[18] T. G. Liu, G. F. Zhao, Y. X. Wang, Phys. Lett. A **375**, 1120 (2011).

[19] W. Qin, W. C. Lu, L. Z. Zhao, Q. J. Zang, C. Z. Wang, K. M. Ho, J. Phys.: Condens. Matter., **21**, 455501 (2009).

[20] J. Wang, J. Zhao, L. Ma, B. Wang, G. Wang, Phys. Lett. A **367**, 335 (2007).

[21] F. C. Chuang, Y.Y. Hsieh, C. C. Hsu, M. A. Albao, J. Chem. Phys. **127**, 144313-1 (2007).

[22] T. T. Cao, L. X. Zhao, X. J. Feng, Y. M. Lei, Y. H. Luo, J. Mol. Struct. Theochem **895**, 148 (2009).

[23] L. J. Guo, X. Liu, G. F. Zhao, Y. H. Luo, J. Chem. Phys. **126**, 234704-1 (2007).

[24] S. Nigam, C. Majumder, S. K. Kulshreshtha, J. Chem. Phys. **121**, 7756 (2004).

[25] C. Xiao, A. Abraham, R. Quinn, F. Hagelberg, W. A. Lester, Jr., J. Phys. Chem. A **106**, 11380 (2002).

[26] J. Wang, Y. Liu, Y. C. Li, Phys. Lett. A **374**, 2736 (2010).

[27] C. Jo, K. Lee, Phys. Lett. A **263**, 376 (1999).

[28] M. Menon, K. R. Subbaswamy, Phys. Rev. B **55**, 9231 (1997).

[29] Z. M. Khakimov, P. L. Tereshchuk, N. T. Sulaymanov, F. T. Umarova, M. T. Swihart, Phys. Rev. B **72**, 115335-1 (2005).

[30] A.M. Mazzone, Comput. Mater. Sci. **39**, 393 (2007).

[31] D. J. Wales, M. C. Waterworth, J. Chem. Soc. Faraday Trans. **88**, 3409 (1992).

[32] R.W. Schmude, Q. Ran, K.A. Gingerich, J.E. Kingcade, J. Chem. Phys. **102**, 2574 (1995).

_____

*Corresponding author: linda_achou@yahoo.fr